NANO LETTERS

LETTER

pubs.acs.org/NanoLett

Spatially Indirect Emission in a Luminescent Nanocrystal Molecule

Charina L. Choi,[†,‡] Hui Li,[§,∥] Andrew C. K. Olson,[†,‡] Prashant K. Jain,[†,‡] Sanjeevi Sivasankar,[*,§,∥] and A. Paul Alivisatos[*,†,‡]

[†]Materials Sciences Division, Lawrence Berkeley National Laboratory, Berkeley, California 94720, United States

[‡]Department of Chemistry, University of California at Berkeley, Berkeley, California 94720, United States

[§]Department of Physics and Astronomy, Iowa State University, Ames, Iowa 50011, United States

[∥]Ames Laboratory, U.S. Department of Energy, Ames, Iowa 50011, United States

Supporting Information

ABSTRACT: Recent advances in the synthesis of multicomponent nanocrystals have enabled the design of nanocrystal molecules with unique photophysical behavior and functionality. Here we demonstrate a highly luminescent nanocrystal molecule, the CdSe/CdS core/shell tetrapod, which is designed to have weak vibronic coupling between excited states and thereby violates Kasha's rule via emission from multiple excited levels. Using single particle photoluminescence spectroscopy, we show that in addition to the expected LUMO to HOMO radiative transition, a higher energy transition is allowed via spatially indirect recombination. The oscillator strength of this transition can be experimentally controlled, enabling control over carrier behavior and localization at the nanoscale.

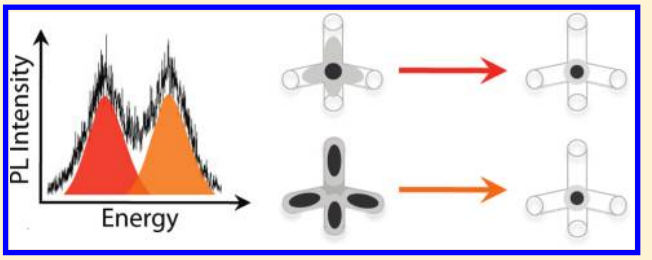

KEYWORDS: Nanocrystal molecule, luminescence, indirect emission, CdSe/CdS core/shell

Kasha's rule is a principle governing luminescence behavior in organic molecules: radiative emission occurs only from the lowest energy excited state of the molecule.[1] This rule follows from kinetic considerations: nonradiative internal conversion between excited states of a given multiplicity is typically fast relative to radiative emission, while internal conversion and radiative emission rates are competitive for relaxation from the lowest excited state to the ground state. Rare molecular exceptions[2] to Kasha's rule exist via decreased nonradiative rates caused by large excited state level spacings, or thermal population of low-lying excited states followed by radiative emission. Highly luminescent nanocrystal molecules,[3] which consist of electronically coupled quantum dot atoms[4−6] typically in a type-I core/shell configuration, also obey Kasha's rule due to relatively fast nonradiative relaxation from higher energy excited states. However, utilizing recent advances in the synthesis of more complex nanocrystal heterostructures, it is conceivable that a nanocrystal molecule with bright photoluminescence may be designed to radiatively emit from multiple excited states to the ground state. Here we demonstrate a nanocrystal molecule, the CdSe/CdS core/shell tetrapod, which breaks Kasha's rule by exhibiting radiative transitions from multiple excited states. Using single particle luminescence spectroscopy, we study the scaling of this violation with experimental parameters and quantify the distribution of energy differences between transitions. We show that in addition to the expected LUMO to HOMO radiative transition, a higher energy transition is allowed via spatially indirect recombination.

The CdSe/CdS core/shell tetrapod is a tetrahedrally symmetric nanocrystal molecule consisting of a zinc blende CdSe quantum dot core and four epitaxially attached CdS arms (Figure 1a,b).[7,8] In analogy to organic molecules, the energy levels of the tetrapod can be described using the language of molecular orbitals, although it is noted that nanocrystal molecule energy levels are not orthogonal. The HOMO of the CdSe/CdS tetrapod involves a hole that is dominantly localized within the central CdSe core, while the LUMO is centered within the core but has a substantial probability of presence in the four arms. The quasi-type-I band alignment of this CdSe/CdS heterostructure results in high luminescence quantum yields of 30−60%.[8] The photoluminescence spectrum from an ensemble of CdSe/CdS tetrapods taken at low excitation fluence exhibits a single emission peak at ∼1.9 eV (Figure 1c), corresponding to emission of an electron into the HOMO level; the peak width of ∼0.12 eV at room temperature is typically considered to be a convolution of the temperature-dependent single particle intrinsic line width and sample polydispersity due to quantum size effects.[5] The ensemble excitation spectrum contains a second higher energy absorption threshold (∼2.4 eV) above the lowest band gap due to absorption in the CdS arms (Figure 1c). At high excitation fluence, emission from the recombination of carriers in CdS may also occur;[9] this is analogous in effect to a molecule containing two uncoupled chromophores.

Received: March 2, 2011
Revised: April 29, 2011
Published: May 19, 2011

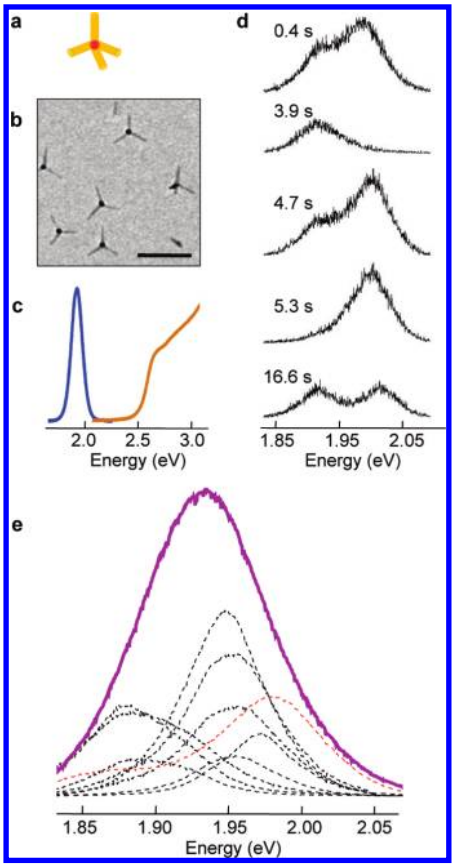

Figure 1. Emission from two discrete energy states is observed in single CdSe/CdS tetrapod nanocrystal molecules. (a) The CdSe/CdS core/shell tetrapod consists of a zinc blende CdSe core (red) with wurtzite CdS arms (yellow). (b) TEM image of CdSe/CdS tetrapods with 30 nm arms. The tetrapods are oriented with three arms on the substrate and the fourth arm protruding out of the plane of the page. (c) Photoluminescence excitation (orange, collected at the emission peak) and emission (blue) spectra from an ensemble of CdSe/CdS tetrapods. (d) Luminescence spectra of a representative 30 nm arm single tetrapod at different time frames (0.1 s integration time). Two emission peaks are clearly seen. (e) The single tetrapod time-integrated emission spectra (dotted curves) summed together (purple curve) reproduce the Gaussian-shaped ensemble fluorescence band; shown here are data for tetrapods with 30 nm arms. Sample traces from singly emitting (black) or multiply emitting (red) single tetrapods are shown for comparison. The amplitude of the ensemble curve is reduced on this plot for clarity.

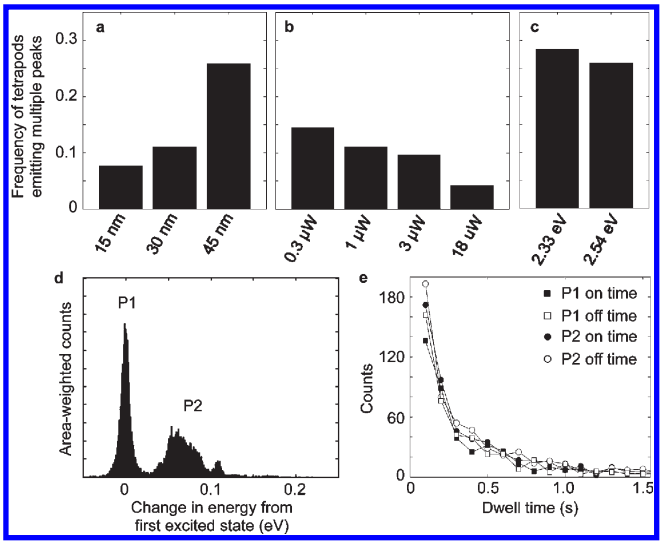

Figure 2. The multiple emission peaks are due to recombination of the CdSe-confined hole with an electron primarily located in either the CdSe or CdS. The fraction of single tetrapods exhibiting multiple peak emission as a function of (a) tetrapod arm length (at 2.54 eV excitation and 1 μW power), (b) incident laser power (for 30 nm arms and 2.54 eV excitation), and (c) excitation wavelength (for 45 nm arms and 1 μW power). (d) Histogram of the energy difference between emission peaks for single tetrapods which emitted radiatively at multiple energies (45 nm arms and 1 μW incident power). This total histogram plot represents data from 18000 spectra from 45 tetrapods. (e) Histogram of the on and off dwell times for the lower (P1) and higher (P2) energy peaks in single tetrapods (45 nm arms and 1 μW incident power).

On the basis of the electronic structure alignment of a CdSe/CdS nanocrystal heterostructure[10,11] and the single particle emission behavior of other semiconductor nanocrystals,[5] it is expected, at least for low excitation fluence, that a single CdSe/CdS tetrapod would emit from only one transition with energy corresponding to the HOMO−LUMO gap of the combined core−shell system. In this Letter, we use single particle luminescence spectroscopy to show that tetrapods can emit radiatively at multiple energies within the spectral range of the CdSe optical band gap (Figure 1d). This behavior is obscured in ensemble measurements due to sample polydispersity and also because a majority of tetrapods exhibit a single radiative transition during the observation time (Figure 1e).

The propensity for radiative transitions from multiple states is affected by several factors, including tetrapod arm length, incident photon fluence, and excitation energy. We studied these effects by measuring the photoluminescence spectra and intensity traces from single tetrapods using a home-built single molecule confocal microscope.[12] Data were collected for tetrapods with 15, 30, or 45 nm arms using 2.33 or 2.54 eV laser excitation at intensities ranging from 0.3 to 18 μW (Methods, Supporting Information). In total, 260400 spectral frames from 651 tetrapods were analyzed.

Tetrapod arm length is an important factor governing the electron wave function delocalization since longer arm lengths increase the probability that an excited electron is located in the CdS arm.[9,13] We found that increasing the tetrapod arm length increased the occurrence of emission from multiple peaks at energies around the CdSe band gap (Figure 2a), suggesting that these multiple emissions were related to an increased occurrence of excited electrons located in the CdS arms. The incident photon flux affects the rate of exciton generation. If multiple peak emission were caused by multiple excitons, we would expect an increase in occurrence with increasing laser intensity;[14] instead we observed a decrease (Figure 2b). The photon energy used to excite the system can alter the spatial origin of carriers due to different band gaps of the heterostructure components; 2.33 eV photon excitation around the CdSe band gap predominantly excites carriers located in the core, whereas photons at 2.54 eV are likely to excite some carriers in the CdS arms as well (Figure 1c). We found that the propensity for multiple radiative transitions was similar regardless of photon energy (Figure 2c), demonstrating that the mechanism for multiple emissions was mostly independent of the spatial origin of excited electrons and holes. Recent studies of single tetrapods at cryogenic temperatures have not revealed multiple luminescence transitions at these energies,[13,15] suggesting that thermal energy also plays a key role in this phenomenon.

dx.doi.org/10.1021/nl2007032 |*Nano Lett.* 2011, 11, 2358–2362

All of the above observations support a model in which the additional radiative transition is caused by spatially indirect emission across the CdSe/CdS heterojunction. Similar behavior has been observed previously in type-II nanocrystal heterostructures in the form of charge-transfer emission.[16−18] The probability of spatially indirect radiative recombination will increase with increasing CdS arm length. Because spatially indirect transitions are slower relative to the rate of direct transitions, increasing the incident photon flux may saturate the indirect channel before the direct channel, resulting in a reduction of the relative yield of indirect transitions.[19,20] Temperature also plays a role in the propensity for the indirect transition: thermal energy at room temperature allows a non-negligible population of electrons in a CdS-dominant excited state, increasing the probability of a spatially indirect emission, regardless of the spatial origin of the carrier.

The energy difference between the multiple emission peaks provides additional insight into the nature of the radiative transitions. An intensity-weighted histogram of the energy of all observed transitions relative to the lowest energy transition shows three peaks (Figure 2d histogram for tetrapods with 45 nm CdS arms; Methods, Figure S3, Supporting Information). The first peak, labeled "P1" and centered around 0 eV, represents emission from the lowest energy transition, while "P2" labels the two remaining peaks on this total histogram: a broader peak around 60 meV and a much smaller, sharper peak around 110 meV. Only two of the 106 total multiply emitting particles exhibited emission at three peaks; most particles exhibited emission from only two states. The existence of two higher energy transitions further supports a model in which additional emissions are caused by spatially indirect transitions. Although a tetrapod is tetrahedrally symmetric, this symmetry is broken when it is immobilized on a substrate; tetrapods preferentially adsorb with three arms slightly bent on the substrate and the fourth arm upright[21] (Figure 1b). Strain from arm bending increases the Cd−S bond lengths especially near the CdSe core, lowering the energy of the CdS conduction band.[22] Thus, the energy of indirect emission from an electron in a strained arm would be lower relative to emission from the upright arm. It is important to note that arm bending induces strain in both the CdSe core and the three bent CdS arms, slightly altering the band structure of both components; only the fourth CdS arm remains unstrained relative to the equilibrium configuration. The lower and higher energy P2 emission peaks can be attributed to transitions involving electrons in the strained and unstrained arms, respectively.

Transition dwell times in and out of both P1 and P2 emission states follow the power law behavior characteristic of blinking from a single emitter[23] (Figure 2e), demonstrating that the duration of luminescence for both radiative transitions is likely dictated by blinking phenomena and also suggesting that the transitions are independent.

The above analysis assumes that the lowest energy transition is the direct transition (Supporting Information), which is likely considering the measured bulk and nanostructured band alignments[10,11] and electronic structure calculations.[9] However, further experiments combining single particle fluorescence spectroscopy with lifetime measurements will allow definitive assignment of emission peak energies to a spatially direct or indirect transition.

The existence of multiple allowed radiative emissions provides another means to probe carrier behavior across a nanoscale heterojunction. From the fluence-dependence data (Figure 2b) we can calculate a radiative lifetime for the spatially indirect

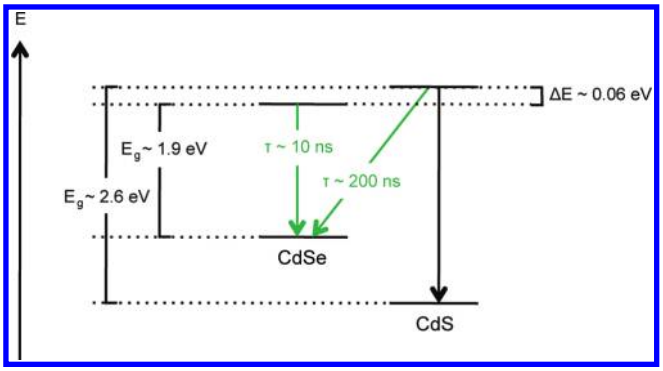

Figure 3. Schematic of the allowed spatially direct and indirect transitions in the CdSe/CdS tetrapod nanocrystal molecule. The LUMO−HOMO transition occurs primarily within the CdSe core, corresponding to a spatially direct recombination. Reduced coupling between the LUMO and the LUMO+1 states due to their small spatial overlap additionally allows radiative emission of an electron from the LUMO+1, located primarily within the CdS arms, to the HOMO, concentrated primarily in the CdSe core (see text). This transition corresponds to a spatially indirect recombination. The lifetime of this transition is calculated to be ~200 ns using the fluence-dependent data (Figure 2b and Supporting Information).

emission (Supporting Information). For a system with a single radiative channel

$$N_{em} = N_{abs}(1 - e^{k/I})\phi$$

where N_{em} is the number of emitted photons, N_{abs} is the number of absorbed photons, k is the radiative rate, I is the rate of incident photons, and ϕ is the intrinsic quantum yield of the transition; $e^{-k/I}$ is the loss of quantum yield from saturation of the recombination channel. By extension of this expression to a two-channel system, using a literature value for $1/k_{direct,CdSe} \leq 1/k_{CdSe\ quantum\ dot} \sim 10$ ns,[24] we calculated a lower limit for the radiative lifetime of $1/k_{indirect,CdS\rightarrow CdSe} \sim 200$ ns (Methods, Supporting Information). This value is in good agreement with reported values of spatially indirect luminescence lifetimes in other systems.[25,26]

A schematic of the allowed transitions in the CdSe/CdS tetrapod nanocrystal molecule is shown in Figure 3. Electronic structure calculations of CdSe/CdS tetrapods[9] show that the LUMO is concentrated in the CdSe core with some probability extending to the CdS arms, while the LUMO+1 is located primarily within each of the four CdS arms. The first 11 hole excited states are confined within the CdSe core. Hence, the hole is expected to undergo relaxation to the HOMO level before radiative recombination can take place. The primary mode of emission is therefore expected to be due to radiative recombination of a CdSe-localized hole (HOMO) with an electron primarily in the CdSe core (LUMO), corresponding to a spatially direct recombination. However, reduced coupling between the LUMO and the LUMO+1 states due to their small spatial overlap can allow radiative recombination of a CdSe-localized hole in the HOMO with an electron largely located within the CdS arms (LUMO+1) before this electron can relax to the LUMO level. The latter corresponds to a spatially indirect recombination. The spatially separated CdSe and CdS components in the tetrapod and the band alignment of the resulting heterostructure create a partially coupled system in which radiative emission from multiple states is allowed.

In this work, we demonstrate at the single particle level that the oscillator strength of the spatially indirect transition can be tuned by changing the arm length of the tetrapod; we predict that the lifetime and energy of this transition can also be altered by appropriate structural modifications. The excited state lifetime of a CdSe/CdS tetrapod increases with arm length;[8,27] the lifetime of the indirect transition should thereby increase as well. A multipod with many CdS arms protruding from a CdSe core might exhibit a spatially indirect transition with the same lifetime as a tetrapod with similar arm lengths, but with increased oscillator strength due to the greater number of arms. A CdSe/CdS tetrapod with extremely thick arms may reduce the quantum confinement in CdS and result in a type II heterostructure,[18,28] changing the energy of the indirect transition. Mechanical strain, which can alter the electronic structure and optical behavior in nanocrystal systems,[22,29,30] may also provide a way to achieve a desired configuration of direct and indirect transitions in a nanocrystal system.

Control over spatially direct and indirect transitions is important for access to both novel fundamental nanoscale behavior and also the rational design of functional systems. Control over carrier localization and transport is extremely important in many applications including photovoltaics and solar-to-fuel. Additionally, multicolor emission within a single highly luminescent particle may provide a unique optical tool. Advances in synthetic techniques to increase the structural and behavioral homogeneity of these complex systems will be crucial efforts toward these goals.

■ ASSOCIATED CONTENT

Supporting Information. Detailed information on methods used and figures showing fluorescence blinking, multiple radiative transitions near the expected CdSe band gap, and energy change histograms from raw emission spectra. This material is available free of charge via the Internet at http://pubs.acs.org.

■ AUTHOR INFORMATION

Corresponding Author

*E-mail: sivasank@iastate.edu; APAlivisatos@lbl.gov.

■ ACKNOWLEDGMENT

H.L. and S.S. thank Dr. Sabyasachi Rakshit and Chi-Fu Yen for help in building the single molecule confocal microscope. Work on nanocrystal synthesis was supported by the Physical Chemistry of Semiconductor Nanocrystals Program, KC3105, Director, Office of Science, Office of Basic Energy Sciences, of the United States Department of Energy under contract DE-AC02-05CH11231. Analysis of single nanocrystal data was supported by the NIH Plasmon Rulers Project NOT-OD-09-056. H.L. and S. S. built the single molecule confocal microscope and were funded by the Grow Iowa Values Fund Award. P.K.J. helped with the single particle analysis and was supported by the Miller Institute through a Miller Fellowship.

■ REFERENCES

(1) Kasha, M. Characterization of electronic transitions in complex molecules. *Discuss. Faraday Soc.* **1950**, *9*, 14–19.

(2) Klán, P.; Wirz, J. *Photochemistry of organic compounds*; Wiley: Chichester, U.K., 2009; Chapter 2, pp 40−41.

(3) Choi, C. L.; Alivisatos, A. P. From artificial atoms to nanocrystal molecules: Preparation and properties of more complex nanostructures. *Annu. Rev. Phys. Chem.* **2010**, *61*, 369–389.

(4) Nirmal, M.; Brus, L. Luminescence photophysics in semiconductor nanocrystals. *Acc. Chem. Res.* **1999**, *32*, 407.

(5) Empedocles, S. A.; Neuhauser, R.; Shimizu, K.; Bawendi, M. G. Photoluminescence from single semiconductor nanostructures. *Adv. Mater.* **1999**, *11*, 1243–1256.

(6) Alivisatos, A. P. Semiconductor clusters, nanocrystals, and quantum dots. *Science* **1996**, *271*, 933–937.

(7) Manna, L.; Milliron, D. J.; Meisel, A.; Scher, E. C.; Alivisatos, A. P. Controlled growth of tetrapod-branched inorganic nanocrystals. *Nat. Mater.* **2003**, *2*, 382–385.

(8) Talapin, D. V.; Nelson, J. H.; Shevchenko, E. V.; Aloni, S.; Sadtler, B.; Alivisatos, A. P. Seeded growth of highly luminescent CdSe/CdS nanoheterostructures with rod and tetrapod morphologies. *Nano Lett.* **2007**, *7*, 2951–2959.

(9) Lutich, A. A.; Mauser, C.; Da Como, E.; Huang, J.; Vaneski, A.; Talapin, D. V.; Rogach, A. L.; Feldmann, J. Multiexcitonic dual emission in CdSe/CdS tetrapods and nanorods. *Nano Lett.* **2010**, *10*, 4646–4650.

(10) Peng, X. G.; Schlamp, M. C.; Kadavanich, A. V.; Alivisatos, A. P. Epitaxial growth of highly luminescent CdSe/CdS core/shell nanocrystals with photostability and electronic accessibility. *J. Am. Chem. Soc.* **1997**, *119*, 7019–7029.

(11) Steiner, D.; Dorfs, D.; Banin, U.; Della Sala, F.; Manna, L.; Millo, O. Determination of band offsets in heterostructure colloidal nanorods using scanning tunneling spectroscopy. *Nano Lett.* **2008**, *8*, 2954–2958.

(12) Sivasankar, S.; Chu, S. Nanoparticle mediated non-fluorescent bonding of microspheres to atomic force microscope cantilevers and imaging fluorescence from bonded cantilevers with single molecule sensitivity. *Nano Lett.* **2009**, *9*, 2120–2124.

(13) Mauser, C.; et al. Spatio-temporal dynamics of coupled electrons and holes in nanosize CdSe-CdS semiconductor tetrapods. *Phys. Rev. B* **2010**, *82*, 081306(R).

(14) Osovsky, R.; Cheskis, D.; Kloper, V.; Sashchluk, A.; Lifshitz, E. Continuous wave pumping of multiexciton bands in the photoluminescence spectrum of a single CdTe-CdSe core-shell colloidal quantum dot. *Phys. Rev. Lett.* **2009**, *102*, 197401.

(15) Borys, N. J.; Walter, M. J.; Huang, J.; Talapin, D. V.; Lupton, J. M. The role of particle morphology in interfacial energy transfer in CdSe/CdS heterostructure nanocrystals. *Science* **2010**, *330*, 1371–1374.

(16) Lo, S. S.; Mirkovic, T.; Chuang, C.-H.; Burda, C.; Scholes, G. D. Emergent properties resulting from type-II band alignment in semiconductor nanoheterostrucures. *Adv. Mater.* **2010**, *23*, 180–197.

(17) Scholes, G. D.; Jones, M.; Kumar, S. Energetics of photoinduced electron-transfer reactions decided by quantum confinement. *J. Phys. Chem. C* **2007**, *111*, 13777–13785.

(18) Donegá, C.d.M. Formation of nanoscale spatially indirect excitons: Evolution of the type-II optical character of CdTe/CdSe heternanocrystals. *Phys. Rev. B* **2010**, *81*, 165303.

(19) Takanohashi, T.; Ozeki, M. Luminescence characteristics of the $(GaP)_n(GaAs)_n$/GaAs atomic layer short-period superlattices. *J. Appl. Phys.* **1992**, *71*, 5614–5618.

(20) Fenigstein, A.; Finkman, E.; Bahir, G.; Schacham, S. E. X-Γ indirect intersubband transitions in type II GaAs/AlAs superlattices. *Appl. Phys. Lett.* **1996**, *69*, 1758–1760.

(21) Liu, H.; Alivisatos, A. P. Preparation of asymmetric nanostructures through site selective modification of tetrapods. *Nano Lett.* **2004**, *4*, 2397–2401.

(22) Smith, A. M.; Mohs, A. M.; Nie, S. Tuning the optical and electronic properties of colloidal nanocrystals by lattice strain. *Nat. Nanotechnol.* **2009**, *4*, 56–63.

(23) Kuno, M.; Fromm, D. P.; Hamann, H. F.; Gallagher, A.; Nesbitt, D. J. Nonexponential "blinking" kinetics of single CdSe quantum dots: A universal power law behavior. *J. Chem. Phys.* **2000**, *112*, 3117–3120.

(24) Califano, M.; Franceschetti, A.; Zunger, A. Temperature dependence of excitonic radiative decay in CdSe quantum dots: the role of surface hole traps. *Nano Lett.* **2005**, *5*, 2360–2364.

(25) Zrenner, A.; et al. Indirect excitons in coupled quantum well structures. *Surf. Sci.* **1992**, *263*, 496–501.

(26) Golub, J. E.; Kash, K.; Harbison, J. P.; Florez, L. T. Long-lived spatially indirect excitons in coupled GaAs/$Al_xGa_{1-x}As$ quantum wells. *Phys. Rev. B* **1990**, *41*, 8564–8567.

(27) Müller, J.; Lupton, J. M.; Lagoudakis, P. G.; Schindler, F.; Koeppe, R.; Rogach, A. L.; Feldmann, J. Wave function engineering in elongated semiconductor nanocrystals with heterogeneous carrier confinement. *Nano Lett.* **2005**, *5*, 2044–2049.

(28) Sitt, A.; Sala, F. D.; Menagen, G.; Banin, U. Multiexciton engineering in seeded core/shell nanorods: Transfer from type-I to quasi-type-II regimes. *Nano Lett.* **2009**, *9*, 3470–3476.

(29) Choi, C. L.; Koski, K. J.; Sivasankar, S.; Alivisatos, A. P. Strain-dependent photoluminescence behavior of CdSe/CdS nanocrystals with spherical, linear, and branched topologies. *Nano Lett.* **2009**, *9*, 3544–3549.

(30) Yang, S.; Prendergast, D.; Neaton, J. B. Strain-induced band gap modification in coherent core/shell nanostructures. *Nano Lett.* **2010**, *10*, 3156–3162.